Journal of the Iranian Chemical Society
https://doi.org/10.1007/s13738-020-01913-2

ORIGINAL PAPER

Molecular docking studies and synthesis of a new class of chroman-4-one fused 1,3,4-thiadiazole derivatives and evaluation for their anticancer potential

L. Kaviarasan[1] · B. Gowramma[1] · R. Kalirajan[1] · M. Mevithra[2] · S. Chandralekha[2]

Received: 4 January 2020 / Accepted: 16 March 2020

Abstract
γ-Secretase inhibitors (GSIs) are repurposed as cancer therapeutics based on the promising inhibition of NOTCH1 signalling pathway in various cancers. GSIs are a class of small-molecule compounds that target the Notch pathway and have been tested to treat various types of cancers in preclinical and clinical trials. Although GSIs elicit a response in some tumours as single agents and sensitize to cytotoxic and targeted therapies, they have not yet been approved for cancer therapy. A new series of chroman-4-one fused 1,3,4-thiadiazole derivatives has been synthesized with the help of different aromatic benzaldehydes, and the final compounds were characterized by FT-IR and ^{1}HNMR. Chroman-4-one fused 1,3,4-thiadiazole derivatives were synthesized by the reaction of Schiff base derivatives with chroman-4-one fused 1,3,4-thiadiazole. All the synthesized compounds were screened for their anticancer activity. These compounds were evaluated for their anticancer activity against MDA-MB-231, MCF-7, and Vero cancer cell lines. Four of the compounds possessed good to moderate anticancer activity. Four of the synthesized compounds, i.e. **3a**, **3c**, **3i**, and **3e,** were found to possess maximum growth inhibition. In conclusion, the designed chromanone-1,3,4-thiadiazole scaffold is an interesting anticancer pharmacophore and considered as novel lead scaffold for any future optimization.

Keywords Chroman-4-one · 1,3,4-thiadiazole · In vitro anticancer · MDA-MB-231 · MCF-7 and Vero cancer cell lines · Gamma secretase inhibitors

Introduction

Among the widespread heterocyclic compounds, oxygen heterocycles occupy a distinct position because of their wide natural abundance and broad biological as well as pharmaceutical significance [1–3]. In these particular classes of O-heterocycles, 'chromone' heterocyclic scaffolds represent a privileged structural motif well distributed in natural products with a broad spectrum of potent biological activities. Chromones as shown in Fig. 1 are benzoannelated γ-pyrone (4H-chromen-4-one, 4H-1-benzopyran-4-one) heterocycles that are widely distributed in nature [4, 5]. They have been used since ancient times in traditional medicine1 and are well known by their diversity of pharmacological properties, such as antiallergic, anti-inflammatory, antidiabetic, antitumor, and antimicrobial [6–8].

The rigid bicyclic chromone fragment has been classified as a privileged structure in drug discovery, due to its use in a wide variety of pharmacologically active compounds such as anticancer, anti-HIV, antibacterial, and anti-inflammatory agents [9–12]. The presence of chromone-based structure in a molecule (Fig. 2) is often associated with its capacity to prevent diseases. Few naturally occurring chromones exhibit antimicrobial, antitumor, antiviral and mutagenic, antiproliferative, and central nervous system (CNS) activities [12–14]. Some chromones are sex pheromones. Numerous synthetic derivatives of naturally occurring chromone have found use in pharmaceuticals, particularly as antifungal and antimicrobial agents [15]. Several chromone derivatives have also been reported to act as kinase inhibitors, to bind to benzodiazepine receptors, and as efficient agents in the

✉ B. Gowramma
gowrammab@jssuni.edu.in

[1] Department of Pharmaceutical Chemistry, JSS College of Pharmacy (JSS Academy of Higher Education and Research, Ooty), Udhagamandalam, Nilgiris, Tamil Nadu 643001, India

[2] Department of Chemistry, PSG College of Arts and Science, Coimbatore, India

Published online: 19 March 2020

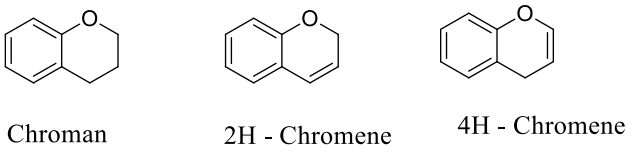

Fig. 1 Structural skeletons of chromones

treatment of cystic fibrosis [16, 17]. A key feature is that the lipophilic nature of the benzopyran derivatives helps to cross the cell membrane easily. Based on the above statement, the present study is based on the antiproliferative activity of chroman-4-one fused 1,3,4-thiadiazole derivatives which were evaluated against various cancer cell lines compared with standard drugs.

Designing of γ-secretase inhibitor

The disruption of oncogenic γ-secretase inhibitor signalling may theoretically be accomplished through various approaches, involving direct and indirect strategies. Many attempts have been carried out to develop γ-secretase inhibitors, including peptidomimetics and non-peptide inhibitors of γ-secretase domain, and inhibitors of the DNA-binding domain of γ-secretases. A strategy is also reported to indirectly block γ-secretases by using modulators of the upstream components of the γ-secretase pathway. Despite many efforts to develop γ-secretase inhibitors, there are no small molecules targeting this protein approved by the FDA so far. In this context, we have tried to identify new chemical fragments to develop more druggable γ-secretase modulators. Based on the literature survey, our group designed a novel chroman-4-one fused 1,3,4-thiadiazole derivative by using SAR. Figure 3 illustrates the newly designed γ-secretase inhibitors.

Results and discussion

In silico docking analysis

Molecular docking was performed to elucidate the binding mode competence of gamma secretase and 25 chromone

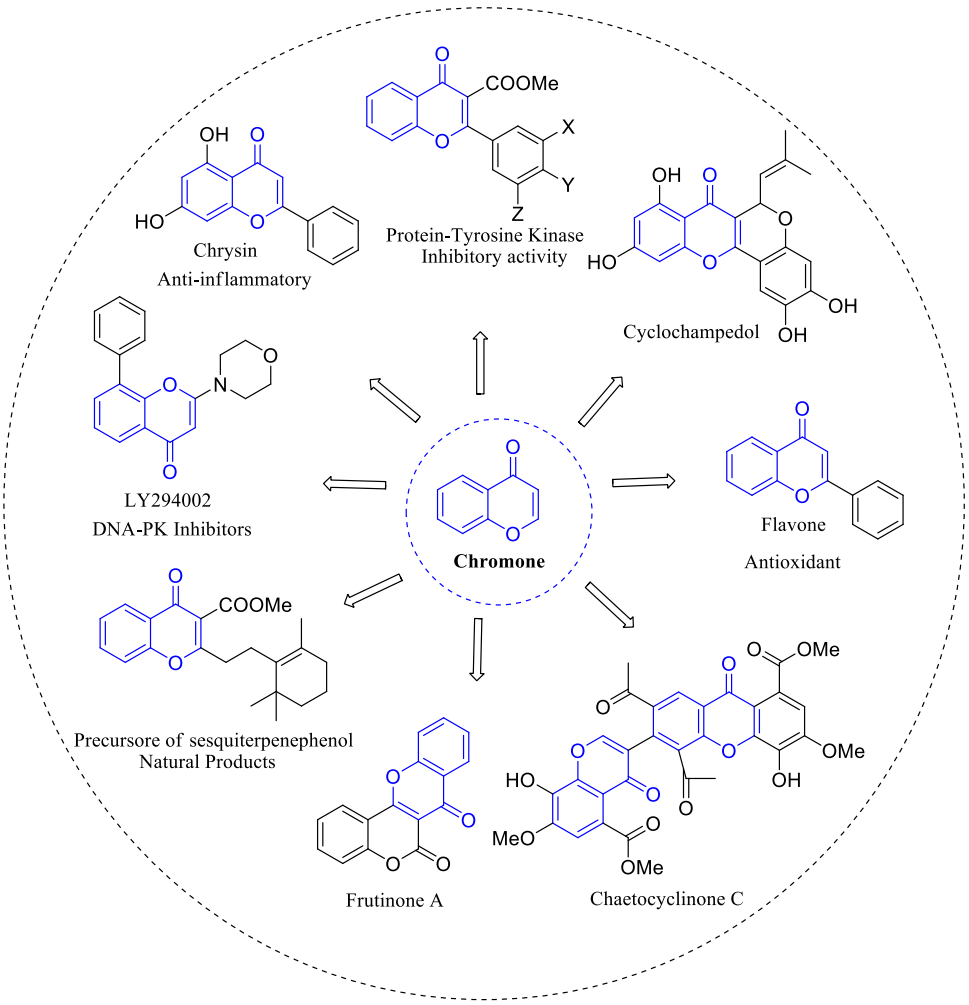

Fig. 2 Natural and synthetic chromone containing heterocyclic compounds

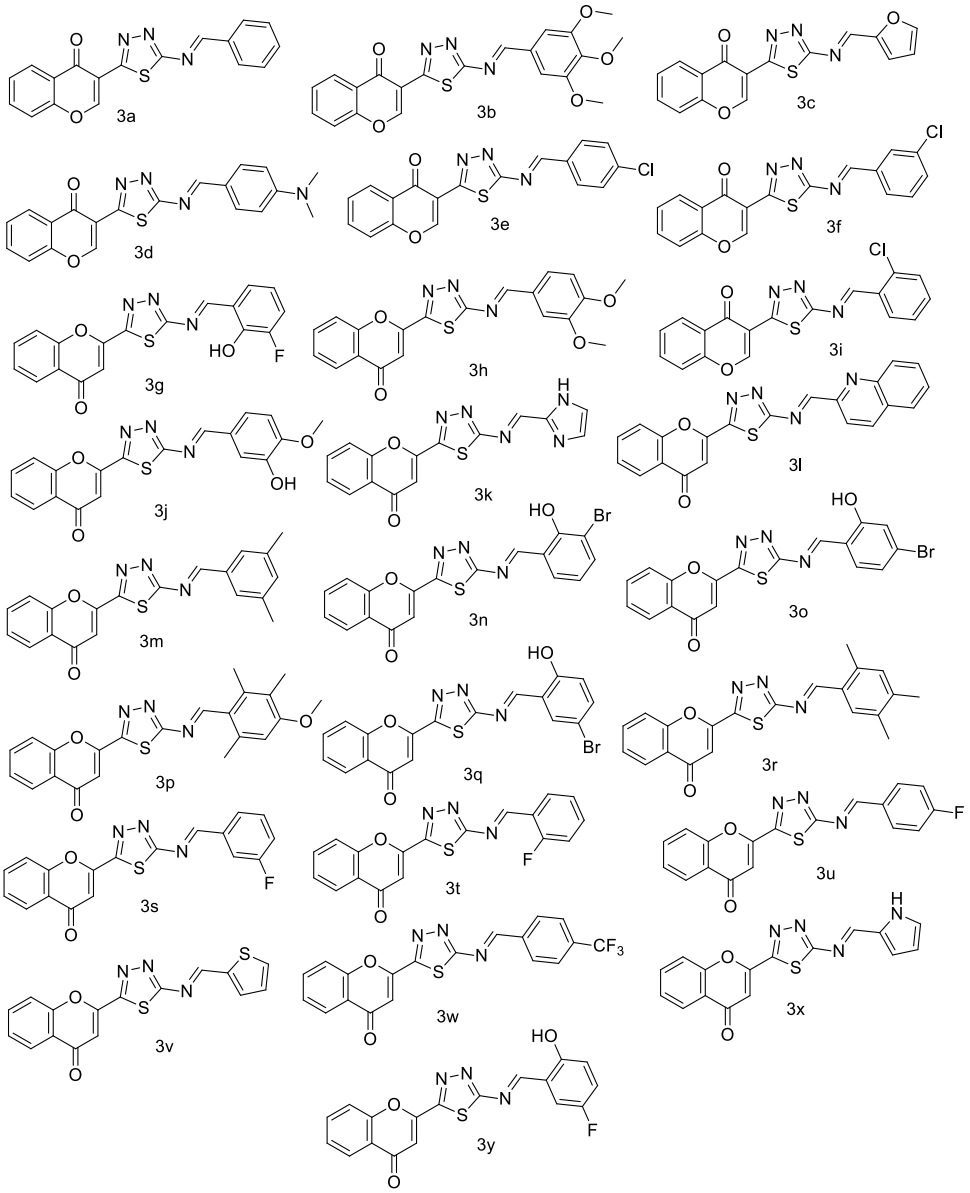

Fig. 3 Newly designed gamma secretase inhibitors

analogues. The designed molecules were docked along with the native ligand and a reference standard, compound **E**. The C dock energy of our designed compounds ranged from 26 to 39 K cal/mol indicated good binding affinities to the target receptor, and the results are depicted in Table 1.

From the docking analysis, compound **3a** (40.37 K cal/mol) has produced better affinity towards active site of gamma secretase enzyme compared to standard drug (42.8599 K cal/mol), and compound **3a** has produced two conventional hydrogen bonds with amino acids Ser A505 and Trp A595, and the chromone ring and thiadiazol ring have produced π–π interaction with amino acid Ser A505 followed by compound **3b** that has better affinity score against targeted enzyme, and this compound has produced conventional two hydrogen bonds with Leu 496. The roles of certain crucial amino acids in the ligand-binding domain of the human gamma secretase inhibitors were also established. Major non-covalent interactions between the studied ligands and the ligand-binding domain of the gamma secretase inhibitors were investigated. These amino acids have been repeatedly implicated during ligand interaction with the gamma secretase inhibitors and also play important role in the inhibition of the ligand-binding domain of gamma secretase inhibitors [18]. These non-covalent interactions, van der Waals, columbic interaction, π–π interaction, and hydrogen interaction, are shown in Fig. 4.

ADMET and toxicity prediction

The 25 molecules obtained after molecular docking studies were subjected to various toxicities and ADMET modules. Log P (an octanol water partition coefficient) is applied as

Table 1 Docking result of designed molecules

Sl. no.	Compound	C docker interaction energy (K cal/mol)
1	STD	42.85
2	**3a**	40.37
3	**3b**	39.61
4	**3c**	38.51
5	**3d**	38.13
6	**3e**	37.46
7	**3f**	37.44
8	**3g**	35.38
9	**3h**	34.75
10	**3i**	34.75
11	**3j**	33.72
12	**3k**	32.57
13	**3l**	32.18
14	**3m**	29.73
15	**3n**	29.72
16	**3o**	29.34
17	**3p**	28.54
18	**3q**	27.46
19	**3r**	27.03
20	**3s**	26.63
21	**3t**	26.48
22	**3u**	25.43
23	**3v**	25.27
24	**3w**	25.24
25	**3x**	24.36
26	**3y**	23.72

significant tool in quantitative structure–activity relationship (QSAR) studies and also in rational drug design as a measure of molecular hydrophobicity; Log P value less than 5 is preferable for drug likeness property. The favourable range of molecular weight is between 320 and 420 g/mol for drug likeness property as stated by Tambunan and Wulandari. Concerning the number of hydrogen bond acceptors (nitrogen or oxygen atoms) and hydrogen bond donors (nitrogen or oxygen atoms with one or more hydrogen atoms), values should be 10 or less than 10 and 5 or less than 5, which agrees with the rule number three and four, respectively. According to rule number five (Lipinski rules), the preferred number of rotatable bonds is 15 or less than 15. Designed ligands of this study have well qualified all the rules of Lipinski's filter (Table 2). Our work has determined various pharmacokinetic and pharmacodynamics properties of newly designed analogues, and the results are represented in Table 3. Pharmacokinetics properties are aqueous solubility and drug likeness, blood–brain barrier penetration (BBB), human intestinal absorption, and cytochrome P450 inhibition. Pharmacodynamics properties (toxicity profile) include aerobic biodegradability, AMES mutagenicity, ocular and skin irritancy, skin sensitizer, and carcinogenicity. Based on result obtained from ADMET module, among 25 examined compounds, ten hits obey all the ADMET properties.

Synthetic work

Based on in silico studies, compound **3a**–**3j** was selected for synthesis. The oxidative cyclization of (E)-2-((4-oxo-4H-chromen-3-yl) methylene) hydrazine carbothioamide (1) synthesized from reaction between 4H-chromen-4-one and thiosemicarbazide, using $POCl_3$ as cyclizing agent, gives 3-(5-amino-1,3,4-thiadiazol-2-yl)-4H-chromen-4-one (2). Further, compound 2 was reacted with different aromatic aldehydes in the presence of methanol to form 3-(5-{[(*Z*)-phenyl substituted] amino}-1,3,4-thiadiazol-2-yl)-2,3-dihydro-4*H*-chromen-4-one from 3-(5-amino, 1,3,4-thiadiazol-2-yl)-4H-chromen-4-one (**3a**–**j**, Scheme 1). All the compounds and intermediates were purified by successive recrystallization from ethanol. The IR spectrum of the final synthesized compounds showed absorption bands around 3300–3156 cm^{-1} for amide NH, while the distinguishing broad absorption peaks C=O for CONH were observed in the range 1720–1690 cm^{-1}, 3350–3157 cm^{-1} for NH, 1489–1464 cm^{-1} for CH_2, 1379–1344 cm^{-1} for CH_3, and 800–700 cm^{-1} for C–S–C. These compounds also exhibited appropriate peaks at corresponding δ ppm in their ^{1}H NMR spectra and corresponding molecular ion peaks in LC–MS spectra which were in conformity with the assigned structures. All the synthesized compounds were subjected for short-term *in vitro* cytotoxicity study.

In vitro anticancer activity

Results of anticancer activity of the compounds were expressed as IC_{50} values which were determined by plotting the percentage cell viability versus concentration of sample on a logarithmic graph and reading off the control. The experiments were performed in triplicates, and then, the final IC_{50} values were calculated by taking average of triplicate experimental results. The study was also carried out with the gamma secretase inhibitor, static. The *in vitro* cytotoxicity study was carried by MTT assay method with cell lines (MDA-MB-231, MCF-7, and Vero-7). All the tested compounds displayed an $IC_{50} > 250$ µg/mL at a concentration range of 30–250 µg/mL. Among the tested compounds, the compound which is substituted with trimethoxy group (**4c**) and the unsubstituted compound (**4d**) displayed considerable anticancer activity against MCF-7 cell line [19, 20]. The results are shown in Table 4.

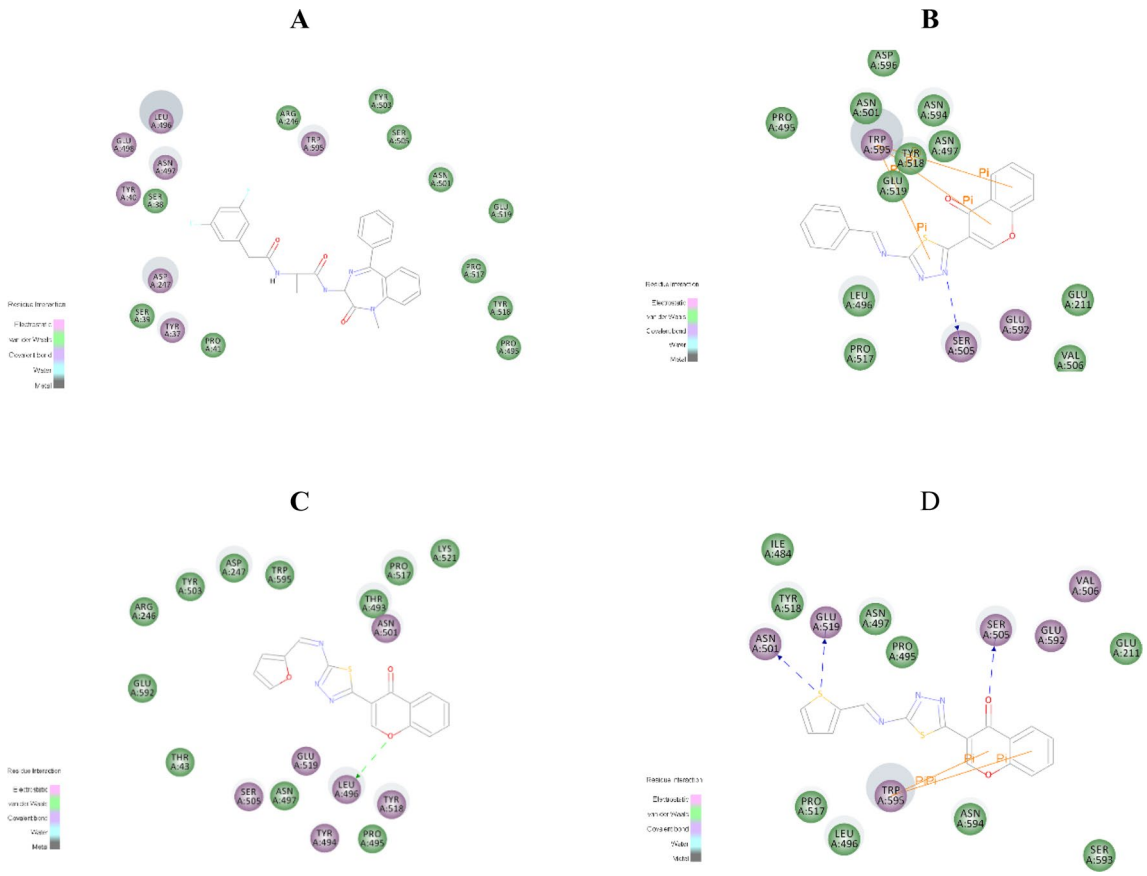

Fig. 4 **a** Docking pose of standard compound **E**; **b** compound **3a**; **c** compound **3c**; **d** compound **3v**

Conclusion

This study has revealed potent gamma secretase inhibitors with good predicted pharmacokinetic profiles that are useful for further investigation for their in vitro as well as in vivo activity towards gamma secretase inhibitor. Structure–activity relationship studies of the substituted chromanone fused 1,3,4-thiadiazole have confirmed that the conformational structure plays an important role in the potency inhibitory activity displayed by chromanone fused 1,3,4-thiadiazole-based compounds in addition to the overall size of the inhibitors. In conclusion, we have developed an efficient methodology to synthesize the derivatives of the title compounds, namely 2-(5-{[(*E*)-(4-nitrophenyl) methylidene] amino}-1,3,4-thiadiazol-2-yl)-4*H*-chromen-4-one. The physicochemical and spectroscopic data confirmed the composition and the structure of the newly synthesized compounds. The investigated molecules are displayed in similar manner of protein binding to the active site of gamma secretase inhibitors (PDB ID: 4R12) on molecular docking studies. The calculated docking energies indicated that its interaction with gamma secretase inhibitors is more favourable but only to a limited extent. All the synthesized compounds were screened for their *in vitro* anticancer activity against MDA-MB-231, MCF-7, and Vero cancer cell lines. All the synthesized compounds were screened for their *in vitro* anticancer activity against MDA-MB-231, MCF-7, and Vero cell line. Among them, compound **3c** and **3j** emerged to be the most active against MDA-MB-231 cell line (IC_{50} = 38.12 and 56.53) and for **3c** and **3e** active against MCF-7 cell line (IC_{50}=41.21 and 66.54) and **3j** and **3a** active against Vero cell line (IC_{50}=42.43 and 47.93) respective cell lines and being more potent for anticancer activity. The study thus serves an attempt to progress towards the discovery of novel anticancer drugs. Additional derivatives may be prepared and further extended for in-depth investigations on other cancer cells so as to establish a SAR (structure–activity relationship) based on rational study. In conclusion, the designed chromanone-1,3,4-thiadiazole scaffold is an interesting anticancer pharmacophore and considered as novel lead scaffold for any future optimization.

Table 2 ADMET result for designed compounds

Name of the compound	H acceptor	H donor	MW	Alog P	Rotatable bond	Polar surface area	AR
3a	5	0	333.36	3.34	3	92.68	3
3b	8	0	423.44	3.29	6	120.37	3
3c	6	0	323.32	2.73	3	105.82	3
3d	6	0	376.43	3.50	4	95.92	3
3e	5	0	367.80	4.0	3	92.68	3
3f	5	0	367.80	4.0	3	92.68	3
3g	6	1	367.35	3.3	3	112.91	3
3h	7	0	393.44	3.13	6	111.14	3
3i	5	0	367.80	4.0	3	92.68	3
3j	7	1	379.38	3.08	4	122.14	3
3k	7	1	323.32	1.63	3	121.36	3
3l	6	0	384.41	3.95	3	105.57	4
3m	5	0	361.41	4.31	3	92.68	3
3n	6	1	428.25	3.85	3	112.91	3
3o	6	1	428.25	3.85	3	112.91	3
3p	6	0	405.47	4.78	4	101.91	3
3q	6	1	428.25	3.85	3	112.91	3
3r	5	0	375.44	4.8	3	92.68	3
3s	5	0	351.35	3.54	3	92.68	3
3t	5	0	351.35	3.5	3	92.68	3
3u	5	0	351.35	3.54	3	92.68	3
3v	5	0	339.39	3.29	3	120.92	3
3w	5	0	401.36	4.28	4	92.68	3
3x	6	1	322.34	2.72	3	108.47	3
3y	6	1	367.35	3.3	3	112.91	3
STD	7	2	490.50	3.77	6	90.87	3

Materials and methods

The melting points were reported using Veego VMP-1 melting point apparatus and LABINDIA digital melting point apparatus expressed in °C and are uncorrected. The reactions performed were monitored by TLC (precoated Merck G_{254}) and detected by UV chamber and iodine as visualizing agent. The IR spectra of the compounds were recorded on Shimadzu FT-IR spectrophotometer using KBr pellets and expressed in cm^{-1}. Nuclear magnetic spectra (^{1}H-NMR) were obtained from Bruker DRX-300 (300-MHz FT-NMR) spectrophotometer using DMSO as solvent with TMS as an internal standard. Mass spectra were recorded on Shimadzu 2010A LC–MS system. All the solvents (AR grade) and reagents were purified and dried according to the standard procedure. In vitro anticancer activity was evaluated using MDA-MB-231, MCF-7, and Vero cancer cell lines.

Molecular docking

The investigated compounds were docked into active site of γ-secretase (PDB ID: 4R12). The procedure was followed by the use of Discovery Studio 4.1 (C docker protocol) software. The crystalline 3D structures of γ-secretase were retrieved from RCSB Protein Data Bank (Fig. 5). The investigated compounds were drawn and saved in mol2 format. Then, the hydrogen bonds were added and the molecule was imported and minimized in Discovery Studio. The obtained structure was saved in PDB format. A final energy minimization was then used to refine the ligand poses. The CDOCKER energy (sum of the internal ligand strain energy and the receptor–ligand non-bonded interaction energy) and CDOCKER interaction energy (the non-bonded interactions between ligand and receptor) were computed for each pose. The interaction and selectivity of the designed compounds were observed for gamma secretase. The docking procedure was validated by extracting ligand CM4 from the binding site and re-docking it to the gamma secretase. The final potential compounds were shortlisted based on the binding pose analysis and dock score [18, 21–24].

Table 3 Toxicity assessment studies of designed compounds

Name	Solubility	AlogP98	BBB	CYP2D6	Hepatotoxic	PPB	PSA 2D
3a	−5.09	0	0.07	−1.43	2.46	2.58	60.07
3b	−4.81	0	−0.36	−2.03	3.11	3.12	86.86
3c	−4.56	0	−0.31	−3.37	1.95	−4.03	72.63
3d	−5.17	0	0.07	−2.40	4.09	4.07	63.42
3e	−5.70	0	0.27	0.68	4.28	6.33	60.07
3f	−4.62	0	−0.27	−1.25	1.73	4.81	77.93
3g	−5.07	0	−0.26	−0.31	4.96	3.41	80.89
3h	−5.71	0	0.27	0.03	3.80	5.76	60.07
3i	−5.72	0	0.27	0.45	2.29	5.86	60.07
3j	−4.75	0	−0.47	−1.49	0.70	1.49	89.82
3k	−3.97	0	−0.87	−3.26	2.81	0.00	86.39
3l	−6.04	0	0.08	−6.32	3.92	4.04	71.33
3m	−6.02	0	0.37	−1.94	1.86	4.24	60.07
3n	−5.53	0	−0.1	−2.46	3.95	2.62	80.89
3o	−5.52	0	−0.1	−2.25	4.77	2.38	80.89
3p	−6.4	0	0.37	−3.13	4.50	8.26	69
3q	−5.54	0	−0.1	−2.25	4.48	1.98	80.89
3r	−6.49	0	0.52	−1.64	2.53	4.54	60.07
3s	−5.31	0	0.13	0.33	5.43	3.47	60.07
3t	−5.32	0	0.13	0.00	4.50	5.40	60.07
3u	−5.3	0	0.13	1.07	5.60	5.81	60.07
3v	−4.85	0	−0.01	−2.63	5.36	4.79	60.07
3w	−6.0	0	0.36	2.07	−2.18	5.33	60.07
3x	−4.84	0	−0.35	−3.23	1.69	0.56	75.13
3y	−5.07	0	−0.26	0.21	7.28	3.14	80.89
STD	−5.14	0	−0.44	−4.76	1.10	4.57	92.19

Aqueous solubility and drug likeness: 0: extremely low; 1: no, but possible; 2: low; 3: good; 4: optimum; 5: too soluble: BBB penetration: 0: very high intensity; 1: high intensity; 2: medium; 3: low. CYP2D6: 0: inhibitor; 1: non-inhibitor

Preparation of the protein

In this step, protein reports are generated to identify potential problems. It involves automatically fixing and building missing loops, optimizes side chains of missing residues, and manages alternate conformations, thus preparing the protein structure, and calculates pK and ionizes at a required pH. After energy minimization and optimization, the obtained protein structure was validated by Ramachandran plot.

Preparation of the ligand molecule

Ligand molecules are prepared by 2D–3D conversion by enumerating ionization state tautomers and isomers. Multiple rapid and exhaustive generation methods are also implicated. Prior to molecular docking, a grid box was generated around the active site of the prepared protein. The docking scores of the designed molecules were compared with compound **E** a known γ-secretase inhibitor under clinical investigation.

ADMET and toxicity prediction

The expectation of drug harmfulness and ADME properties is significant filtration standard for the drug design process. Subsequently, adsorption, distribution, metabolism, excretion, and toxicity (ADMET) which is identified with pharmacokinetics are significant parameters considered during the drug development process. Different scientific prescient ADMET pharmacokinetic parameters, for example blood–brain–barrier penetration, human intestinal absorption, aqueous solubility, cytochrome P4502D6 inhibition, hepatotoxicity, and plasma protein binding, were determined quantitatively for the selected 25 ligands utilizing ADMET modules in Discovery Studio v4.1 customer [25].

Scheme 1 General procedure for synthesis of title compounds

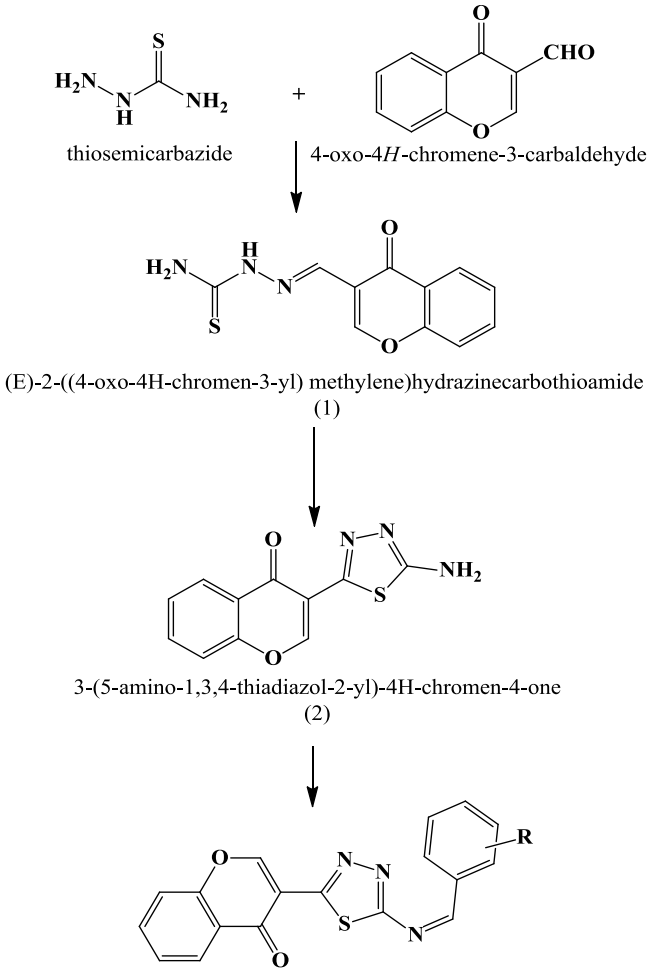

Benzaldehyde (3a), 3,4,5-Trimethoxy benzaldehyde (3b), Furfural (3c), 4-Dimethylaminobenzaldehyde 3d), 4-Chloro benzaldehyde (3e), 3-Chloro benzaldehyde (3f), 3-Fluroro 2 hydroxy benzaldehyde (3g), 3,4-Dimethoxybenzaldehyde (h), 2,Cholro benzaldehyde (3i), 3- Hydroxy-4-methoxybenzaldehyde (3j)

Table 4 In vitro cytotoxic evaluation of synthesized compounds against MDA-MB-231, MCF-7, and Vero cell lines

Name of the compound	MDA-MB-231 (IC_{50} µg/mL)	MCF-7 (IC_{50} µg/mL)	Vero (IC_{50} µg/mL)
3a	70.22	98.23	47.93
3b	125.66	75.47	57.12
3c	38.12	41.21	30.21
3d	> 250	168.87	> 150
3e	114.16	66.54	76.23
3f	123.39	88.27	145.31
3g	158.57	76.54	156.77
3h	174.03	142.78	189.92
3i	108.57	96.54	126.77
3j	56.53	78.34	42.43

Chemistry

Synthesis of (E)-2-(4-oxo-4H-chromen-3-yl) methylene) hydrazine carbothioamide (1)

3-formyl chromone (0.435) was dissolved in 50 mL of warm ethanol, and thiosemicarbazide (0.22 gm) was dissolved in 50 mL of hot water, and they were mixed slowly with continuous stirring. The product is separated by filtration after cooling. The completion of reaction was monitored by TLC using ethyl acetate: hexane (5:5) as mobile phase. The melting point was reported, and the recrystallization was carried out by ethanol.

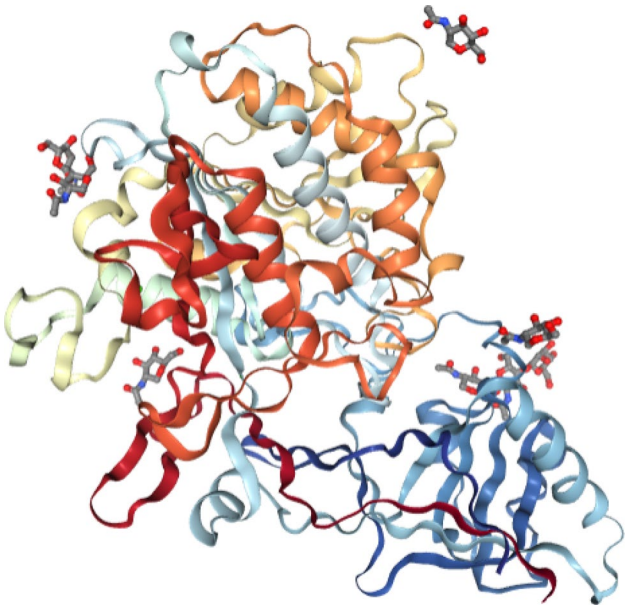

Fig. 5 Crystal structure of γ-secretase (4R12)

Synthesis of 3-(5-amino-1,3,4-thiadiazol-2-yl)-4H-chromen-4-one (2)

2.45 gm of thiosemicarbazide derivative (1) was refluxed for 6 h in concentrated sulphuric acid. After 6 h, the reaction mixture was poured into crushed ice. The precipitate was filtered off and crystallized from ethanol. The completion of reaction was monitored by TLC using ethyl acetate: hexane (5:5) as mobile phase.

Synthesis of 3-(5-{[(Z)-phenyl substituted] amino}-1,3,4-thiadiazol-2-yl)-2,3-dihydro-4H-chromen-4-one from 3-(5-amino, 1,3,4-thiadiazol-2-yl)-4H-chromen-4-one (3a–J)

A mixture of compound 2 (00.1 mol), methanol (30 mL), and aromatic aldehyde (00.1 mol) was reflexed on water bath at 90 °C for 6 h (Scheme 1). The contents were then poured onto crushed ice; the resulting solid was filtered and recrystallized using DMF 60%. The completion of reaction was monitored by TLC using ethyl acetate: hexane (4:6) as mobile phase.

Synthesis of (Z)-3-(5-(benzylideneamino)-1,3,4-thiadiazol-2-yl)-4H-chromen-4-one (3a) A mixture of compound 2 (2.45 gm), methanol (30 mL), and benzaldehyde (1.06 gm) was reflexed on water bath at 90 °C for 6 h. The contents were then poured onto crushed ice; the resulting solid was filtered and recrystallized using ethanol. The completion of reaction was monitored by TLC using ethyl acetate: hexane (4:6) as mobile phase. $C_{18}H_{13}N_3O_2S$; reddish orange crystal; MP: 199–200 °C; yield 61.2%; solvent for crystallization : ethanol; IR (cm^{-1}): 1388.17(C–O–C), 1652.1(C=O), 1595.98(C=N), 3363.93(N=C), 878.86(C–H); ^{1}H NMR (DMSO-d_6, 400 MHz, δ ppm): 8.68 (1H, *s*), 8.36 (1H, *s*), 8.08 (1H, *d*), 7.83 (2H, *d*), 7.55 (2H, *d*), 7.47 (1H, *t*); ^{13}C NMR: 175.3, 160.0, 157.2, 135.2, 131.0, 125.8, 129.2, 116.2; *m/z*: 334.42 (333 gm). Anal. Calcd for $C_{18}H_{13}N_3O_2S$: C, 64.85; H, 3.33; N, 12.60; O, 9.60; S, 9.62; Found: C, 62.14; H, 2.73; N, 10.91; O, 10.52; S, 11.21.

Synthesis of (E)-2-(5-((2,4,5-trimethoxybenzylidene) amino)-1,3,4-thiadiazol-2-yl)-4H-chromen-4-one (3b) A mixture of compound 2 (2.45 gm), methanol (30 mL), and 2,4,5-trimethoxy benzaldehyde (1.96 gm) was reflexed on water bath at 90 °C for 6 h. The contents were then poured onto crushed ice; the resulting solid was filtered and recrystallized using ethanol. The completion of reaction was monitored by TLC using ethyl acetate: hexane (4:6) as mobile phase. $C_{21}H_{19}N_3O_5S$; deep red colour solid; MP: 249–250 °C; yield: 61%; solvent for crystallization: ethanol; IR (cm^{-1}): 1326.85 (C–O–C), 1654.54(C=O), 1583.21(C=N), 3451.55 (N=C imine), 845.80(C–H). ^{1}H NMR (DMSO-d_6, 400 MHz, δ ppm): 8.36 (1H, *s*), 8.08 (1H, *d*), 7.55 (2H, *d*), 7.47 (1H, *t*), 6.71 (1H, *s*), 6.41 (1H, *s*), 3.83 (6H, *s*); ^{13}C NMR: 177.5, 168.8, 160.0, 158.9, 156.2, 135.2, 123.9, 123.4, 110.23, 108.98, 98.45, 56.84; *m/z*: 422.61 (423 gm). Anal. Calcd for $C_{21}H_{19}N_3O_5S$: C, 59.57; H, 4.05; N, 9.92; O, 18.89; S, 7.57: Found: C, 56.83; H, 5.49; N, 10.59; O, 20.13; S, 6.78.

Synthesis of (Z)-2-(5-((furan-2-ylmethylene)amino)-1,3,4-thiadiazol-2-yl)-4H-chromen-4-one (3c) A mixture of compound 2 (2.45 gm), methanol (30 mL), and furfuraldehyde (0.96 gm) was reflexed on water bath at 90 °C for 6 h. The contents were then poured onto crushed ice; the resulting solid was filtered and recrystallized using ethanol. The completion of reaction was monitored by TLC using ethyl acetate: hexane (4:6) as mobile phase. $C_{16}H_9N_3O_3S$; yellow colour solid; MP: 278–279 °C, yield: 78%; solvent for crystallization: ethanol; IR cm^{-1}: 1353.10 (C–O–C), 1652.26 (C=O), 1580.61(C=N), 3452.03 (N=C imine), 8464.39 (C–H). ^{1}H NMR (DMSO-d_6, 400 MHz, δ ppm): 8.08 (1H, *d*), 7.75 (1H, *d*), 7.55 (2H, *d*), 7.50 (1H, *s*), 6.71 (1H, *s*); 6.52 (1H, *d*); ^{13}C NMR: 177.5, 168.8, 160.0, 158.9, 156.2, 144.21, 146.52, 135.2, 123.9, 123.4, 112.98, 110.23. *m/z*: 323.67 (323 gm). Anal. Calcd for $C_{16}H_9N_3O_3S$: C, 59.44; H, 2.81; N, 13.00; O, 14.85; S, 9.92: Found: C, 56.29; H, 3.10; N, 10.24; O, 16.93; S, 10.91.

Synthesis of (Z)-3-(5-(4-(dimethylamino)benzylidene) amino)-1,3,4-thiadiazol-2-yl)-4H-chromen-4-one (3d) A mixture of compound 2 (2.45 gm), methanol (30 mL), and dimethylamino benzaldehyde (1.49 gm) was reflexed on

water bath at 90 °C for 6 h. The contents were then poured onto crushed ice; the resulting solid was filtered and recrystallized using ethanol. The completion of reaction was monitored by TLC using ethyl acetate: hexane (4:6) as mobile phase. $C_{20}H_{16}N_4O_2S$; brown colour solid; MP: 329–330 °C; yield: 75%; solvent for crystallization: Ethanol; Ethanol; IR (cm^{-1}): 1382.65(C–O–C), 1652.54(C=O), 1599.01(C=N), 3333.43(N=C), 870.28(C–H); ^{1}H NMR (DMSO-d_6, 400 MHz, δ ppm): 8.68 (1H, *s*), 8.36 (1H, *s*), 8.08 (1H, *d*), 7.83 (2H, *d*), 7.55 (2H, *d*), 7.47 (1H, *t*); ^{13}C NMR: 175.3, 160.0, 157.2, 135.2, 131.0, 125.8, 129.2, 116.2; *m/z*: 377. Anal. Calcd for $C_{20}H_{16}N_4O_2S$: C, 63.81; H, 4.28; N, 14.88; O, 8.50; S, 8.52: Found: C, 61.01; H, 3.54; N, 15.68; O, 9.64; S, 6.84.

Synthesis of (Z)-3-(5-((4-chlorobenzylidene) amino)-1,3,4-thiadiazol-2-yl)-4H-chromen-4-one (3e) A mixture of compound 2 (2.45), methanol (30 mL), and 4-chloro benzaldehyde (1.4 gm) was reflexed on water bath at 90 °C for 6 h. The contents were then poured onto crushed ice; the resulting solid was filtered and recrystallized using ethanol. The completion of reaction was monitored by TLC using ethyl acetate: hexane (4:6) as mobile phase. $C_{18}H_{10}N_3O_2SCl$; reddish brown colour solid; MP: 315–316 °C; yield: 75%; solvent for crystallization: Ethanol; Ethanol; IR (cm^{-1}): 1339.15 (C–O–C), 1654.54(C=O), 1583.21(C=N), 3447.55 (N=C imine), 865.80 (C–H). ^{1}H NMR (DMSO-d_6, 400 MHz, δ ppm): 8.68 (1H, *s*), 8.59 (1H, *s*), 8.08 (1H, *d*), 7.77 (1H, *d*), 7.55 (2H, *d*), 7.52 (1H, *t*), 7.47 (2H, *d*); ^{13}C NMR:182.59, 175.30, 160.55, 135.31, 136.64, 125.21, 125.90; *m/z*: 368.0. Anal. Calcd for $C_{18}H_{10}N_3O_2SCl$: C, 58.78; H, 2.74; Cl, 9.64; N, 11.42; O, 8.70; S, 8.72: Found: C, 56.26; H, 5.21; Cl, 7.27; N, 10.67; O, 6.86; S, 5.95.

Synthesis of (Z)-3-(3-chlorobenzylidene) amino)-1,3,4-thiadiazol-2-yl)-4H-chromen-4-one (3f) A mixture of compound 2 (2.45 gm), methanol (30 mL), and 3-chloro benzaldehyde (1.4 gm) was reflexed on water bath at 90 °C for 6 h. The contents were then poured onto crushed ice; the resulting solid was filtered and recrystallized using ethanol. The completion of reaction was monitored by TLC using ethyl acetate: hexane (4:6) as mobile phase. $C_{18}H_{10}N_3O_2SCl$; yellow colour solid; MP: 312–313 °C; yield: 79%; solvent for crystallization: Ethanol; Ethanol; IR (cm^{-1}): 1282.33 (C–O–C), 1636.74 (C=O), 3023.94(=CH), 850.25 (C–H aromatic ring); ^{1}H NMR (DMSO-d_6, 400 MHz, δ ppm): 8.68 (1H, *s*), 8.59 (1H, *s*), 8.33 (2H, *d*), 7.07 (1H, *d*), 7.55 (2H, *d*), 7.52 (1H, *t*), 7.47 (2H, *d*); ^{13}C NMR:180.29, 175.30, 160.45, 159.27, 150.25, 142.60, 135.24, 127.21, 116.90; *m/z*: 368. Anal. Calcd for $C_{18}H_{10}N_3O_2SCl$: C, 58.78; H, 2.74; Cl, 9.64; N, 11.42; O, 8.70; S, 8.72: Found: C, 56.26; H, 5.21; Cl, 7.27; N, 10.67; O, 6.86; S, 5.95.

Synthesis of (E)-2-(5-((3-fluoro-2-hydroxybenzylidene) amino)-1,3,4-thiadiazol-2-yl)-4H-chromen-4-one (3g) A mixture of compound 2 (2.45 gm), methanol (30 mL), and 3-fluoro-2-hydroxy benzaldehyde (1.4 gm) was reflexed on water bath at 90 °C for 6 h. The contents were then poured onto crushed ice; the resulting solid was filtered and recrystallized using ethanol. The completion of reaction was monitored by TLC using ethyl acetate: hexane (4:6) as mobile phase. $C_{18}H_{10}N_3O_3SF$; yellowish colour solid; MP: 312–313 °C; yield: 79%; solvent for crystallization: Ethanol; Ethanol; IR (cm^{-1}): 1372.14 (C–O–C), 1661.54 (C=O), 1450.01(C=N), 3333.43(N=C), 870.28(C–H); ^{1}H NMR (DMSO-d_6, 400 MHz, δ ppm): 8.68 (1H, *s*), 8.59 (1H, *s*), 7.55 (2H, *d*), 7.52 (1H, *t*), 7.47 (2H, *d*), 5.35 (1H, *s*); ^{13}C NMR: 180.59, 175.91, 161. 18, 159.96, 159.27, 150.25, 142.60, 135.24, 127.21, 116.90; *m/z*: 367. Anal. Calcd for $C_{18}H_{10}N_3O_3SF$: C, 58.85; H, 2.74; F, 5.17; N, 11.44; O, 13.07; S, 8.73: Found: C, 56.57; H, 3.21; F, 4.39; N, 10.11; O, 11.57; S, 8.01.

Synthesis of (E)-2-(5-((3,4-dimethoxybenzylidene) amino)-1,3,4-thiadiazol-2-yl)-4H-chromen-4-one (3h) A mixture of compound 2 (2.45 gm), methanol (30 mL), and 3,4-dimethoxy benzaldehyde (1.6 gm) was reflexed on water bath at 90 °C for 6 h. The contents were then poured onto crushed ice; the resulting solid was filtered and recrystallized using ethanol. The completion of reaction was monitored by TLC using ethyl acetate: hexane (4:6) as mobile phase. $C_{19}H_{13}N_3O_3S$; dark red colour solid; MP: 291–292 °C; yield: 75%; solvent for crystallization: Ethanol; Ethanol; IR (cm^{-1}): 1326.85 (C–O–C), 1654.54(C=O), 1583.21(C=N), 3451.55 (N=C imine), 845.80(C–H). ^{1}H NMR (DMSO-d_6, 400 MHz, δ ppm): 8.36 (1H, *s*), 8.08 (1H, *d*), 7.55 (2H, *d*), 7.47 (1H, *t*), 6.71 (1H, *s*), 6.41 (1H, *s*), 3.83 (3H, *s*); ^{13}C NMR: 177.5, 168.8, 160.0, 158.9, 156.2, 135.2, 123.9, 123.4, 110.23, 108.98, 98.45, 56.84; *m/z*: 393. Anal. Calcd for $C_{19}H_{13}N_3O_3S$: C, 61.06; H, 3.84; N, 10.68; O, 16.27; S, 8.15: Found: C, 60.30; H, 2.98; N, 8.92; O, 15; S, 14.76.

Synthesis of (Z)-3-(5-((2-chlorobenzylidene) amino)-1,3,4-thiadiazol-2-yl)-4H-chromen-4-one (3i) A mixture of compound 2 (2.45 gm), methanol (30 mL), and 2-chloro benzaldehyde (1.4 gm) was reflexed on water bath at 90 °C for 6 h. The contents were then poured onto crushed ice; the resulting solid was filtered and recrystallized using ethanol. The completion of reaction was monitored by TLC using ethyl acetate: hexane (4:6) as mobile phase. $C_{18}H_{10}N_3O_2SCl$; reddish brown colour solid; MP: 326–327 °C; yield: 72%; solvent for crystallization: ethanol; IR (cm^{-1}): 1339.15 (C–O–C), 1654.54(C=O), 1583.21(C=N), 3447.55 (N=C Imine), 865.80 (C–H). ^{1}H NMR (DMSO-d_6, 400 MHz, δ ppm): 8.68 (1H, *s*), 8.59 (1H, *s*), 8.08 (1H, *d*), 7.77 (1H, *d*), 7.55 (2H, *d*), 7.47 (2H, *d*); ^{13}C NMR:182.59, 175.30,

160.55, 135.31, 136.64, 125.21, 125.90; *m/z*: 368. Anal. Calcd for $C_{18}H_{10}N_3O_2SCl$: C, 58.78; H, 2.74; Cl, 9.64; N, 11.42; O, 8.70; S, 8.72: Found: C, 56.26; H, 5.21; Cl, 7.27; N, 10.67; O, 6.86; S, 5.95.

Synthesis of (E)-2-(5-((3-hydroxy-4-methoxybenzylidene) amino)-1,3,4-thiadiazol-2-yl)-4H-chromen-4-one (3j) A mixture of compound 2 (2.45 gm), methanol (30 mL), and 3-hydroxy-4-methoxy benzaldehyde (1.52 gm) was reflexed on water bath at 90 °C for 6 h. The contents were then poured onto crushed ice; the resulting solid was filtered and recrystallized using ethanol. The completion of reaction was monitored by TLC using ethyl acetate: hexane (4:6) as mobile phase. $C_{19}H_{13}N_3O_4S$; reddish brown colour solid; MP: 321–322 °C; yield: 72%; solvent for crystallization: ethanol; IR (cm^{-1}): 1353.60(C–O–C), 1654.49(C=O) 1595.98 (C=N), 3253.16(N=C imine) 878.86(C–H). ^{1}H NMR (DMSO-d_6, 400 MHz, δ ppm): 8.68 (1H, *s*), 8.59 (1H, *s*), 8.08 (1H, *d*), 7.77 (1H, *d*), 7.55 (2H, *d*), 5.35 (2H, *d*), 3.83 (1H, *d*); ^{13}C NMR:182.59, 175.30, 160.55, 135.31, 136.64, 125.21, 125.90; *m/z*: 379. Anal. Calcd for $C_{19}H_{13}N_3O_4S$: C, 60.15; H, 3.45; N, 11.08; O, 16.87; S, 8.45: Found: C, 58.51; H, 2.15; N, 10.57; O, 15.82; S, 7.34.

In vitro anticancer activity

The *in vitro* cytotoxicity of the synthesized compounds was assessed against MDA-MB-231, MCF-7, and Vero cancer cell lines. The monolayer culture of the cell line was trypsinized, followed by adjusting the cell count to 1.0×10^5 cells/mL by means of DMEM medium containing 10% FBS. The diluted cell suspension (0.1 mL) was added to each well of the 96-well microtiter plate. The test wells were added with various concentrations (100 µL) of test samples, and the control wells received media (100 µL). The plates were then incubated at 37 °C for 72 h in 5% CO_2 atmosphere. After this duration, the cultures were fixed with trichloroacetic acid (25 µL, 10% w/v) and stained for 30 min with sulforhodamine B (0.4% w/v) in acetic acid (1% v/v). Unbound dye was cleared by four washes with acetic acid (1% v/v), and protein-bound dye was extracted with 10 mM unbuffered Tris base [tris (hydroxymethyl) aminomethane]. The optical density of the protein-bound dye was recorded at 540 nm. The percentage cell viability (CV) was calculated using the following formula:

$$\text{Cell viability} = \frac{\text{Mean OD of individual test group}}{\text{Mean OD of control group}} \times 100$$

The concentration of test samples required to inhibit cell growth by 50% was tabulated from the dose–response for each cell line.

Acknowledgements The authors are grateful to 'His Holiness Jagadguru Sri Shivarathree Deshikendra Mahaswamigalavaru' of Sri Suttur Mutt, Mysore, for providing facilities to carry out this work. We also thank our Pro Chancellor Dr. B. Suresh, JSS Academy of Higher Education and Research, Mysore, Management of JSS College of Pharmacy, Udhagamandalam, Department of Pharmacology, Biotechnology and Pharmaceutical Analysis, for their technical support.

Compliance with ethical standards

Conflict of interest The authors declare that there are no conflicts of interest.

References

1. E. Alipour, Z. Mousavi, Z. Safaei, M. Pordeli, M. Safavi, L. Firoozpour, M. Mohammadhosseini, M. Saeedi, S. Kabudanian Ardestani, A. Shafiee, A. Foroumadi, Daru J. Pharm. Sci. **22**, 22–41 (2014)
2. B.H. Alizadeh, M. Saeedi, D. Dehghan, A. Foroumadi, A. Shafiee, J. Iran. Chem. Soc. **12**, 605–612 (2015)
3. B.H. Alizadeh, S.N. Ostad, A. Foroumadi, M. Amini, R. Dowlatabadi, L. Navidpour, A. Shafiee, ARKIVOC **13**, 45–56 (2008)
4. J.K. Boulamwini, H. Assefa, J. Med. Chem. **45**(4), 841–852 (2002)
5. A. Boumendjel, J. Boccard, P. Carrupt, E. Nicolle, M. Blanc, M. Geze, L. Choisnard, D. Wouessidjewe, E. Matera, C. Dumontet, J. Med. Chem. **51**(7), 2307–2310 (2008)
6. A.K. Brien, R.K. Bandi, A.K. Behera, B.K. Mishra, P. Majumdar, V. Satam, M. Savagian, S. Tzou, M. Lee, M. Zeller, A.J. Robles, S. Mooberry, H. Pati, Arch. Pharm. Chem. Life Sci. **345**, 341–348 (2012)
7. S. Demirayak, L. Yurttas, N. Gundogdu Karaburun, A.C. Karaburun, I. Kayagil, J. Enzyme Inhib. Med. Chem. **30**, 816–825 (2015)
8. S. Demirayak, L. Yurttas, N. Gundogdu Karaburun, A.C. Karaburun, I. Kayagil, Lett. Drug Des. Discov. **13**, 563–569 (2016)
9. J.R. Dimmock, M.P. Padmanilyam, G.A. Zello, J.W. Quail, E.O. Oloo, J.S. Prisciak, H.B. Kraatz, B. Cherkasov, J.S. Lee, T.M. Allen, C.L. Santos, E.K. Manavathu, E. De Clercq, J. Balzarini, J.B. Eur, J. Med. Chem. **37**, 813–824 (2002)
10. S. Emami, Z. Ghanbarimasir, Eur. J. Med. Chem. **26**, 539–563 (2015)
11. A.M. Gamal Eldeen, A. Abdel Lateff, T. Okino, Toxicol. Pharmacol. **28**, 317–322 (2009)
12. Y. Gao, Q. Ren, H. Wu, M. Li, J. Wang, Chem. Commun. (Cambridge) **46**(48), 9232–9234 (2010)
13. H.I. Gul, K.O. Yerdelen, M. Gul, U. Das, B. Pandit, P.K. Li, H. Secen, F. Sahin, Arch. Pharm. **340**, 195–201 (2007)
14. N. Gundogdu Karaburun, A.C. Karaburun, S. Demirayak, I. Kayagil, L. Yurttas, Lett. Drug Des. Discov. **11**, 578–585 (2014)
15. A. Husain, M. Rashis, A. Shaharyar, A.A. Siddiqui, R. Mishra, Eur. J. Med. Chem. **62**, 785–798 (2013)
16. L. Ivanova, L. Varinska, M. Pilatova, P. Gal, P. Solar, P. Perjesi, K. Smetana, A. Ostro, Mol. Biol. Rep. **40**, 4571–4580 (2013)
17. R.S. Keri, S. Budagumpi, P.K. Pai, R.G. Balakrishna, Eur. J. Med. Chem. **78**, 340–374 (2014)
18. T. SchulzGasch, M. Stahl, J. Mol. Mod. **9**, 47–57 (2003)
19. B. Gowramma, T.K. Praveen, S. Gomathy, B. Babu, R. Kalirajan, N. Krisnaveni, Curr. Bioact. Compd. **14**(3), 309–316 (2018)
20. B. Gowramma, S. Krishna, M. Mohammed, T.K. Praveen, R. Kalirajan, L. Kaviarasan, Lett. Drug Des. Discov. **17**(4), 432–442 (2020)

21. H.B. Kwon, C. Park, K.H. Jeon, E. Lee, S.E. Park, K.Y. Jun, T.M. Kadayat, P. Thapa, R. Karki, Y. Na, M.S. Park, S.B. Rho, E.S. Lee, Y. Kwon, J. Med. Chem. **58**, 1100–1122 (2015)
22. E.M. Krovat, T. Steindl, T. Langer, Curr. Comput. Aided Drug Des. **1**, 93–102 (2005)
23. P. Ferrara, H. Gohlke, D.J. Price, G. Klebe, C.L. Brooks, J. Med. Chem. **47**, 3032–3047 (2004)
24. M. Kontoyianni, L.M. McClellan, G.S. Sokol, J. Med. Chem. **47**, 558–565 (2004)
25. B. Kupcewicz, A.A. Jarzecki, M. Małecka, U. Krajewska, M. Rozalski, Bioorg. Med. Chem. Lett. **24**, 4260–4265 (2014)